Gaseous $[N_2O_5]H^+$, $[N_2O_4]H^+$, and Related Species from the Addition of NO_2^+ and NO^+ Ions to Nitric Acid and Its Derivatives

Fernando Bernardi,*,† Fulvio Cacace,‡ Giulia de Petris,*,‡ Federico Pepi,‡ and Ivan Rossi†

Dipartimento di Chimica "G.Ciamician", Università di Bologna, via Selmi, 2, 40126 Bologna, Italy, and Dipartimento di Studi di Chimica e Tecnologia delle Sostanze Biologicamente Attive, Università di Roma "La Sapienza", p.le A.Moro, 5, 00185 Rome, Italy

Received: November 5, 1997; In Final Form: December 31, 1997

Gaseous $[HN_2O_5]^+$ ions formed upon addition of NO_2^+ to nitric acid have been studied by mass spectrometric and computational methods. The results from MIKE, CAD and FT-ICR spectrometry and calculations at the B3LYP 6-311++G(3df, 3dp)//6-311G(d,p) level of theory show that the most stable adduct formed is an electrostatic $HNO_3 \cdot NO_2^+$ complex where NO_2^+ is coordinated to the nitro group of nitric acid. Consequently, the nitro group is the energetically preferred protonation site of N_2O_5, whose experimental proton affinity (PA) amounts to 189.8 ± 2 kcal mol^{-1}, vs theoretically computed values ranging from 182 to 188 kcal mol^{-1}. Addition of NO_2^+ to XNO_2 molecules (X = CH_3O, C_2H_5O and NH_2) also yields electrostatic complexes where the nitronium ion is coordinated to the NO_2 group. The most stable $[HN_2O_4]^+$ ion from the addition of NO^+ to HNO_3 is also identified as a cluster characterized by coordination of the nitrosonium ion to the nitro group, whose almost thermoneutral isomerization into a cluster where a nitronium ion is coordinated to the nitroso group of HNO_2 is characterized by a sizable barrier. The larger PA of N_2O_5 than of H_2O and HNO_3 is of interest in atmospheric chemistry, pointing to protonation by H_3O^+ and/or $H_2NO_3^+$ ions as the first step of the N_2O_5 destruction in ionic clusters and aerosols.

Introduction

Gas-phase positive ion chemistry of nitric acid and related molecules is the focus of sustained interest, owing to its intrinsic fundamental interest[1] and the relevance to atmospheric chemistry.[2−6] Particular attention has been devoted to protonated nitric acid, both in the isolated state and in water clusters,[7−18] and the investigation has been extended to its derivatives, i.e., protonated alkyl nitrates[19−22] and nitramide,[23] leading to the construction of a scale of NO_2^+ binding energies (BE).[24]

Among the nitric acid derivatives examined, a conspicuous exception is N_2O_5, whose positive ion chemistry is virtually unexplored, except concerning the measurement of its ionization potential.[25−27] This is surprising, in view of the importance of N_2O_5 to the chemistry of the upper atmosphere, where it represents a reservoir molecule for the NO_x oxides involved in the ozone cycle and contributes to the formation of nitric acid and organic nitrates.[28−30] Given the role played by N_2O_5 in atmospheric chemistry, there is a considerable interest in the reactions responsible for its formation and decomposition. As to the latter process, it has been suggested that it may be promoted by proton transfer to N_2O_5 from hydrated H_3O^+ ions within ionic clusters and/or aerosols, followed by conversion into HNO_3,[29,30] via the likely intermediacy of protonated N_2O_5.

In this article we report the results of a joint experimental and computational study of the positive ion chemistry of N_2O_5 and related species, focusing attention on their protonation and alkylation. A central problem concerns the preferred site of the cation attachment, for example, isomeric species can be formed, upon protonation of N_2O_5

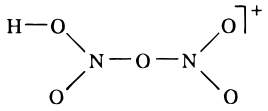

1a

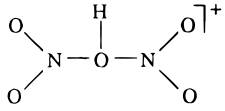

2a

An interesting aspect is that there are two different routes to the above cations, namely, direct proton transfer from gaseous acids of adequate strength

$$N_2O_5 \xrightarrow[-A]{+HA^+} [HN_2O_5]^+ \qquad (1)$$

or addition of NO_2^+ to appropriate molecules, for example

$$NO_2^+ + HNO_3 \rightarrow [HN_2O_5]^+ \qquad (2)$$

Nitration of nitric acid, the reverse of the process postulated for the acid-catalyzed decomposition of N_2O_5, is intrinsically interesting and provides a link between the basicity of N_2O_5 and the nucleophilicity of HNO_3, in that the relative stability of **1a** and **2a** can be viewed as reflecting either the local proton affinity (PA) of the basic sites of N_2O_5 or the local NO_2^+ BE of the nucleophilic centers of HNO_3. Species of the general formula $[XN_2O_4]^+$, where X = CH_3O, C_2H_5O, and NH_2 were also studied to investigate the influence of the substituent X on the stability of isomeric adducts.

The study was extended to the related reaction

$$NO^+ + HONO_2 \rightarrow [HN_2O_4]^+ \qquad (3)$$

whose product, nitrosated nitric acid, is liable to conversion into nitrated nitrous acid, an intracomplex process of potential interest to atmospheric chemistry.

† Università di Bologna.
‡ Università di Roma.

S1089-5639(98)00084-X CCC: $15.00
Published on Web 02/24/1998

TABLE 1: MIKE Spectra of Relevant Species

ion	formation[a] process	labeled reagent	fragment[b] *m/z* (relative intensity, %)
$[HN_2O_5]^+$	(1)		46 (100)
$[DN_2O_5]^+$	(1)	D_3^+	46 (100)
$[HN_2O_5]^+$	(2)		46 (100)
$[HN^{15}NO_5]^+$	(2)	$H^{15}NO_3$	46 (100)
$[CH_3N_2O_5]^+$	(6)		46 (100)
$[CH_3N_2O_5]^+$	(7)		46 (100)
$[CH_3N_2O_4{}^{18}O]^+$	(7)	$NO^{18}O^+$	46 (39); 48 (61)
$[CH_3N_2O_3{}^{18}O_2]^+$	(7)	$N^{18}O_2^+$	46 (43); 50 (57)
$[CH_3N^{15}NO_5]^+$	(7)	$^{15}NO_2^+$	46 (38); 47 (62)
$[C_2H_5N_2O_5]^+$	(12)		46 (100)
$[C_2H_5N_2O_5]^+$	(13)		46 (100)
$[C_2H_5N_2O_4{}^{18}O]^+$	(13)	$NO^{18}O^+$	46 (46); 48 (54)
$[C_2H_5N_2O_3{}^{18}O_2]^+$	(13)	$N^{18}O_2^+$	46 (46); 50 (54)
$[C_2H_5N^{15}NO_5]^+$	(13)	$^{15}NO_2^+$	46 (39); 47 (61)
$[H_2N_3O_4]^+$	(14)		46 (100)
$[H_2N_2{}^{15}NO_4]^+$	(14)	$^{15}NO_2^+$	46 (100)
$[HN_2O_4]^+$	(18)		30 (100)
$[HN^{15}NO_4]^+$	(18)	$^{15}NO^+$	31 (100)

[a] The numbers in parentheses correspond to those of the reactions in the text. [b] Standard deviation of the relative intensities ±10%.

TABLE 2: CAD Spectra of Relevant Species

ion	fragment[a] *m/z* (relative intensity %)
$[HNO_3NO_2]^+$	30 (5.7); 46[b](92.9); 63 (1.4)
$[H^{15}NO_3NO_2]^+$	30 (5.5); 31 (7.8); 46[b](74.6); 47 (10.4); 64 (1.7)
$[N_2O_5H]^+$	30 (6.9); 46[b](90.4); 63 (2.7)
$[N_2O_5D]^+$	30 (7.3); 46[b](90.2); 64 (2.5)
$[HNO_3NO]^+$	30[b](70.8); 46(25.4); 63(3.8)
$[HNO_3{}^{15}NO]^+$	30(8.0); 31[b](66.2) 46(18.8); 47(3.2); 63(3.8)
$[CH_3ONO_2NO_2]^+$	30 (4.1); 46[b](95.9)
$[N_2O_5CH_3]^+$	30 (4.3); 46[b](95.7)
$[C_2H_5ONO_2NO_2]^+$	29 (2.3); 30 (2.4); 46[b](90.7); 76 (4.6)
$[N_2O_5C_2H_5]^+$	29 (2.2); 30 (4.0); 46[b](89.6); 76 (4.2)
$[H_2N\ NO_2\ NO_2]^+$	30 (9.0); 46[b](81.9); 62 (9.1)

[a] The ions were prepared in the same way as in Table 1. Standard deviation of relative intensities ±10%. [b] Fragment formed also by unimolecular dissociation; see Table 1.

Mass Spectrometric Results

The structure, or more precisely the connectivity of the ions from the protonation and alkylation of N_2O_5 and from the nitration and nitrosation of HNO_3 and its derivatives, was examined by mass-analyzed ion kinetic energy (MIKE) and collisionally activated dissociation (CAD) spectrometries, whereas the NO_2^+ BE of HNO_3 was evaluated by the kinetic method.[31] Supporting evidence on the structure of the nitrated ions was sought by examining their reactivity by Fourier-transform ion cyclotron resonance (FT-ICR) mass spectrometry. The results obtained from the joint application of the above techniques to the characterization of the species assayed are outlined in the following paragraphs.

$[HN_2O_5]^+$ Ions. Table 1 summarizes the MIKE spectra of the ions prepared according to reaction 1 by H_2O/CI and D_2/CI of N_2O_5 and according to reaction 2 by CH_3ONO_2/CI of HNO_3. The MIKE spectra are almost identical in both cases, displaying only the metastable loss of NO_2^+, $m/z = 46$, even when $H^{15}NO_3$ is nitrated with NO_2^+ according to reaction 2. This favors structure **1a**, showing that the $^{15}NO_2$ and the NO_2 groups of the decomposing ions *are not equivalent*, as would be the case for protomer **2a**. The CAD spectra of $[HN_2O_5]^+$ ions from reactions 1 and 2, reported in Table 2, are also identical, displaying again NO_2^+ as the major charged fragment, whose origin, however, is not entirely collisional, owing to the unimolecular contribution, apparent from the data of Table 1. The CAD spectrum of the $[HN^{15}NO_5]^+$ ions obtained utilizing $H^{15}NO_3$ in reaction 2 is particularly informative, showing that unlabeled NO_2^+ accounts for nearly 90% of nitronium ions lost and hence that the NO_2 and $^{15}NO_2$ groups of $[HN^{15}NO_5]^+$ *are not equivalent*. This is supported by the collision-induced loss of $H^{15}NO_3^+$, $m/z = 64$, but not of HNO_3^+, $m/z = 63$.

Both MIKE and CAD spectrometries provide strong evidence that $[HN_2O_5]^+$ ions, at the moment of their structural assay, have the connectivity typical of structure **1a**, irrespective of their formation process. This inference is consistent with the results from the experiments aimed at measuring the NO_2^+ BE of HNO_3 according to the kinetic method.[31] In fact, it has been found that the $[HN_2O_5L]^+$ adducts, where L denotes a suitable ligand, obtained by CH_4/CI of N_2O_5/L mixtures, or by NO_2/CI of HNO_3/L mixtures, behave exactly in the same way and are to be regarded as $[HNO_3(NO_2^+)L]$ nitronium ion-bound dimers whose unimolecular dissociation occurs exclusively according to the competing processes

$$[HNO_3(NO_2^+)L] \xrightarrow{k_4} HNO_3NO_2^+ + L \quad (4)$$

$$[HNO_3(NO_2^+)L] \xrightarrow{k_5} LNO_2^+ + HNO_3 \quad (5)$$

Significantly, the k_4/k_5 branching ratio for a given ligand is the same irrespective of whether the adduct is obtained from protonated N_2O_5 or nitrated HNO_3, and furthermore, when $N^{18}O_2$/CI is used, only $N^{18}O_2+$ is transferred to the L ligand, showing that the two NO_2 units are not equivalent, which is only consistent with the presence of protomer **1a** in the dimer. This specific application is remarkably free of the complications frequently encountered in the utilization of the kinetic method, i.e., reactions 4 and 5 are not accompanied by other fragmentation processes. In addition, the evaluation of the NO_2^+ BE of representative ligands has been the subject of a detailed study, which provides a most useful base for the choice of the experimental parameters and the data analysis.[24] To evaluate the NO_2^+ BE of HNO_3 by the kinetic method, a reference ligand of known, and sufficiently low, BE is required. Since the lowest BE reported, that of H_2O, is too large to allow direct application of the method to the H_2O/HNO_3 pair, we must use another suitable ligand. To this end, the NO_2^+ BE of CH_3F has been evaluated to be 19.0 ± 2 kcal mol^{-1} by utilizing the calibration factor previously adopted for 18 ligands.[24] In turn, application of the kinetic method to the CH_3F/HNO_3 pair gives a NO_2^+ BE of HNO_3 of 18.3 ± 2 kcal mol^{-1}, which according to the general correlation valid for n-type nucleophilic centers[24] would correspond to a PA of the nitrated site amounting approximately to 161 kcal mol^{-1}. Such a close, if partially fortuitous, agreement with the PA of the NO_2 group of HNO_3, which according to CCDS(T) calculations[12] amounts to 161.2 ± 4 kcal mol^{-1}, provides additional, albeit indirect, evidence for the assignment of structure **1a** to $[HN_2O_5]^+$ ions. In this connection, on the basis of the above correlations,[24] the 182 kcal mol^{-1} PA of HNO_3, which refers to protonation of the OH group, would lead to a NO_2^+ BE of such group amounting to 23.1 ± 2 kcal mol^{-1}, well in excess of the experimental value, 18.3 ± 2 kcal mol^{-1}, providing additional evidence against structure **2a**.

On the basis of a thermochemical cycle involving the measured $HNO_3-NO_2^+$ BE, the heats of formation of H^+ and NO_2^+, and those of HNO_3 and N_2O_5, one arrives at a PA(N_2O_5) of 189.8 ± 3 kcal mol^{-1}.

In summary, the experimental results show that, irrespective of their origin, the $[HN_2O_5]^+$ populations, when subjected to

structural analysis, i.e., ca. 10 ms after their formation, consist predominantly, if not exclusively, of ions having the connectivity typical of protomer **1a**. This can hardly be traced to a high site selectivity of their formation processes, i.e., protonation of N_2O_5 and nitration of HNO_3, and is likely to reflect the operation of processes occurring after the formation of the $[HN_2O_5]^+$ ions, i.e., fast **2a** → **1a** isomerization and/or fast dissociation of any **2a** ions initially formed owing to the low NO_2^+ BE of the OH group of HNO_3.

$[CH_3N_2O_5]^+$ Ions. Two reactions were employed for the preparation of the ions, namely the alkylation

$$(CH_3)_2F^+ + N_2O_5 \rightarrow [CH_3N_2O_5]^+ + CH_3F \qquad (6)$$

performed by CH_3F/CI and the nitration

$$NO_2^+ + CH_3ONO_2 \rightarrow [CH_3N_2O_5]^+ \qquad (7)$$

performed by NO_2/CI. The MIKE and CAD spectra of the ions from reactions 6 and 7 are indistiguishable, in that only metastable loss of NO_2^+ is observed (Table 1), whereas collisional dissociation yields, in addition, only NO^+ (Table 2). These results do not allow structural discrimination between the conceivable isomers

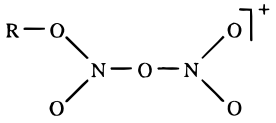

1b R = CH_3, **1c** R = C_2H_5

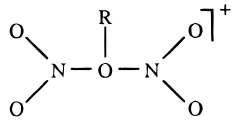

2b R = CH_3, **2c** R = C_2H_5

The MIKE spectra of the labeled ions obtained by utilizing $N^{18}O_2^+$ ($^{15}NO_2^+$) in reaction 7 show a comparable loss of NO_2^+ and $N^{18}O_2^+$ ($^{15}NO_2^+$), with a small but significant preference for the loss of the labeled fragment (Table 1). Such a pattern would suggest that the decomposing ions are a mixed **1b**/**2b** population, where the isomer **2b** predominates.

When reactions 6 and 7 are performed in the presence of a suitable ligand L, one obtains $[CH_3N_2O_5L]^+$ adducts whose MIKE spectra are undistinguishable and characterize the ions as $[CH_3ONO_2(NO_2^+)L]$ nitronium ion-bound dimers. In fact, the processes giving the $CH_3ONO_2NO_2^+ + L$ and the $LNO_2^+ + CH_3ONO_2$ fragments pairs are the only metastable transitions observed. Utilizing CH_3F and $CH_2(CN)_2$ as the reference ligands, the NO_2^+ BE of CH_3ONO_2 was found to amount to 20.7 ± 2 kcal mol^{-1}, which according to the above-cited BE/PA correlation[24] leads to a local PA of the nitrated site of CH_3ONO_2 of ca. 171 kcal mol^{-1}. This is close to the 172 ± 3 kcal mol^{-1} value calculated at the CCSD(T) level of theory[13] for the NO_2 group of methyl nitrate, which provides indirect evidence for structure **1b**. This inference is supported by the MIKE spectra of the $[CH_3ONO_2(N^{18}O_2^+)L]$ dimers prepared from reaction 7 utilizing $N^{18}O_2$. Irrespective of the NO_2^+ BE of the specific ligand utilized, only the labeled nitronium ion is transferred; for example, one observes the metastable decomposition

$$[CH_3ONO_2(N^{18}O_2^+)CH_3CN] \rightarrow CH_3CN(N^{18}O_2)^+ + CH_3ONO_2 \qquad (8)$$

but not the corresponding process involving NO_2^+ transfer. In short, the evidence from the study of nitronium ion-bound dimers suggests that they contain a $[CH_3N_2O_5]^+$ unit having the connectivity typical of isomer **1b**.

Further evidence was sought by Fourier-transform ion cyclotron resonance mass spectrometry. $H_2O{\cdot}N^{18}O_2^+$ ions, obtained by $N^{18}O_2$/CI of H_2O in the external ion source of the spectrometer, were isolated by selective ejection techniques and driven into the resonance cell containing CH_3ONO_2 and a strong nucleophile, CH_3CN.

The labeled ions from the ligand exchange

$$H_2ON^{18}O_2^+ + CH_3ONO_2 \rightarrow CH_3ONO_2N^{18}O_2^+ + H_2O \qquad (9)$$

were isolated, and their reaction with the nucleophile was monitored. Both nitronium ion-transfer processes

$$CH_3ONO_2N^{18}O_2^+ + CH_3CN \rightarrow CH_3CN(N^{18}O_2)^+ + CH_3ONO_2 \qquad (10)$$

$$CH_3ONO_2N^{18}O_2^+ + CH_3CN \rightarrow CH_3CN(NO_2)^+ + CH_3ON^{18}O_2 \qquad (11)$$

occur at comparable rate, suggesting that the ionic population assayed consists predominanty, or exclusively, of isomer **2b**.

The situation is less than clear-cut, in that the evidence from MIKE and FT-ICR experiments involving isolated $[CH_3N_2O_5]^+$ ions points to the predominance of isomer **2b**, whereas MIKE experiments, involving nitronium ion-bound adducts, suggest instead the exclusive presence of isomer **1b**. A reasonable explanation is that the ligand L catalyzes the conversion of **2b** into **1b**, which is selectively stabilized by differential solvation by L within the long-lived ion neutral complex.[32] Such interpretation presupposes, of course, that the stability difference between the isomers be small.

$[C_2H_5N_2O_5]^+$ Ions. Two processes were utilized for these preparation, namely, alkylation

$$C_2H_5^+ + N_2O_5 \rightarrow [C_2H_5N_2O_5]^+ \qquad (12)$$

by CH_4/CI of N_2O_5 and nitration by NO_2/CI

$$NO_2^+ + C_2H_5ONO_2 \rightarrow [C_2H_5N_2O_5]^+ \qquad (13)$$

The ions from both reactions display the same MIKE and CAD spectra (Tables 1 and 2), and their $[C_2H_5N_2O_5L]^+$ adducts with neutral ligands L behave as $[C_2H_5ONO_2(NO_2)^+L]$ nitronium ion-bound dimers. The picture outlined by the mass spectrometric experiments is analogous to that typical of $[CH_3N_2O_5]^+$ ions, and the same considerations apply. Utilizing $C_2H_5NO_2$ and $CH_2(CN)_2$ as the reference ligands, application of the kinetic method leads to a NO_2^+ BE of 22.8 ± 2 kcal mol^{-1}, corresponding to a PA of the nitrated site of ca. 180 kcal mol^{-1} according to the above cited BE/PA correlation.[24]

$[H_2N_3O_4]^+$ Ions. Direct nitration of nitramide

$$NO_2^+ + H_2NNO_2 \rightarrow [H_2N_3O_4]^+ \qquad (14)$$

was utilized for their preparation. The only metastable transition observed is the loss of NO_2^+, $m/z = 46$ (Table 1), whereas only the $^{15}NO_2^+$ fragment, $m/z = 47$, is lost from the ions obtained utilizing $^{15}NO_2^+$ in reaction 14. The CAD spectrum (Table 2) is also informative, showing in addition to the loss of the NO_2^+ the $H_2N_2O_2^+$ fragment at m/z 62. Finally, FT-ICR experiments were performed, whereby $H_3N^{15}NO_2^+$ ions, produced in the external ion source upon ionization of a $^{15}NO_2/NH_3$ mixture were isolated and driven into the resonance cell containing CH_3-

ONO_2 and a nucleophile, CH_3CN. The labeled ions formed via the process

$$H_3N^{15}NO_2^+ + CH_3ONO_2 \rightarrow [H_2N^{15}NO_2NO_2]^+ + CH_3OH \quad (15)$$

a general reaction to be discussed in a forthcoming paper,[33] were isolated and allowed to react with the nucleophile. Significantly, only the unlabeled NO_2 group is transferred

$$[H_2N^{15}NO_2NO_2]^+ + CH_3CN \rightarrow H_2N^{15}NO_2 + CH_3CN(NO_2)^+ \quad (16)$$

$$[H_2N^{15}NO_2NO_2]^+ + CH_3CN \not\rightarrow H_2NNO_2 + CH_3CN(^{15}NO_2)^+ \quad (17)$$

The failure to detect process 17 shows, consistent with the MIKE and CAD results, that the two NO_2 groups within $[H_2N_3O_4]^+$ are not equivalent and favors structure **1d** over **2d**

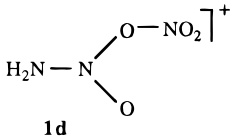

1d

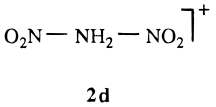

2d

$[HN_2O_4]^+$ Ions. Their preparation involved direct nitrosation of HNO_3 by NO/CI

$$NO^+ + HNO_3 \rightarrow [HN_2O_4]^+ \quad (18)$$

The MIKE spectra of the ion, and of its labeled counterpart obtained utilizing $^{15}NO^+$ in reaction 18, do not allow discrimination between the conceivable structures

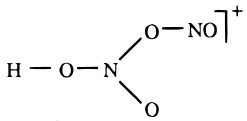

3

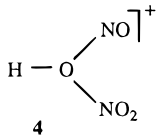

4

In fact, the observed loss of NO^+ (Table 1) rather than of NO_2^+ does not provide, in this case, evidence for isomer **3**, in that it could reflect as well a higher barrier to the metastable loss of NO_2^+ than of NO^+ in isomer **4**. The CAD spectra (Table 2) are more informative, especially with regard to the detection of a small but significant $^{15}NO_2^+$ fragment at $m/z = 47$ from $[HN^{15}NO_4]^+$, which is more consistent with structure **3**.

The $[HN_2O_4L]^+$ adducts from the NO/CI of HNO_3/L mixtures have a complex metastable fragmentation pattern where the dissociation as nitrosonium ion-bound dimers

$$[HNO_3(NO^+)L] \xrightarrow{k_{19}} HNO_3NO^+ + L \quad (19)$$

$$[HNO_3(NO^+)L] \xrightarrow{k_{20}} LNO^+ + HNO_3 \quad (20)$$

is accompanied by other processes. Nevertheless, utilizing H_2O and CH_3Cl as the reference ligands and the calibration side from a comprehensive study of NO^+ BE,[34] application of the kinetic method leads to a NO^+ BE of HNO_3 amounting to 17.1 ± 2 kcal mol^{-1}. On the basis of the general NO^+ BE/PA correlation,[34] the estimated PA of the nitrosated site of HNO_3 would be 160.2 kcal mol^{-1}, which favors protomer **3**, in that the calculated[12] local PA of the NO_2 group of HNO_3 is very close, 161.2 ± 4 kcal mol^{-1}. In conclusion, the mass spectrometric results seem to favor structure **3**, albeit the assignment should be regarded as tentative.

Further indirect support is provided by the published values of the NO^+ BE to CH_3ONO_2 and $C_2H_5ONO_2$, i.e., 20.7 ± 2 and 22.7 ± 2 kcal mol^{-1}, respectively.[34] Utilizing the above-cited NO^+ BE/PA correlation, one can estimate the PA of the nitrosated site to amount to ca. 170 kcal mol^{-1} in CH_3ONO_2 and 175.5 kcal mol^{-1} in $C_2H_5ONO_2$. These values are remarkably close to the computed PA of the NO_2 group in CH_3ONO_2 and $C_2H_5ONO_2$, 172 ± 3 [13] and 177.0 kcal mol^{-1},[22] respectively, which favors the NO_2-protonated isomer **3**. Albeit the evidence is indirect, the trend holds for all $RONO_2$ species examined (R = H, CH_3, C_2H_5), which makes a fortuitous agreement rather unlikely.

Computational Results

Nitrogen oxides present a relatively difficult computational problem since their correct description require both a high-level treatment of dynamic electron correlation and large basis sets. Ab initio methods such as the coupled cluster, while being very accurate, become rapidly very expensive with the increase of the number of atoms in the molecular system studied. A good compromise between speed and accuracy is represented by methods based on density functional theory such as B3LYP,[35,36] as also recently shown by Smith and Radom[37] by comparing the ability of several ab initio and density functional methods to calculate proton affinities.

In this paper we studied the $[HN_2O_5]^+$ and $[HN_2O_4]^+$ ions by means of the B3LYP hybrid density functional. Geometry optimizations and harmonic frequency calculations were performed at the B3LYP/6-311G(d,p) level for all the structures studied. To minimize the effect of basis set incompleteness, the electronic energies were then recomputed by single-point calculations on the optimized structures using the larger 6-311++G(3df, 3pd) basis set (Tables 3 and 4). All the calculations were performed using the GAUSSIAN 94 program suite.[38]

To test the performance of the method, we computed the local proton affinities of the $-OH$ and $-NO_2$ sites of HNO_3 and the binding energy for the $NO_2^+ \cdot H_2O$ cluster, which is the most stable isomer of $[H_2NO_3]^+$. We obtain local proton affinities of 175.9 and 160.2 kcal mol^{-1}, respectively and a binding energy of 17.4 kcal mol^{-1} at 298 K. The most recent experimental values are $PA(HNO_3) = 182.0 \pm 2.3$ kcal mol^{-1} and $BE = 19.6 \pm 2.4$ kcal^{-1} mol,[15] whereas the best computational values to date are 182.5 ± 4 and 161.2 ± 4 kcal mol^{-1}, respectively, for the local proton affinities (298 K) and 17.3 ± 2 kcal mol^{-1} (0 K) for the binding energy, calculated by Lee and Rice[12] at the coupled-cluster CCSD(T) level of theory. We can then conclude that the density functional approach used compares reasonably well with both the experimental and the computational results.

$[HN_2O_5]^+$ Ions. For the $[HN_2O_5]^+$ ion we found two stable structures, denoted as **II** and **III** in Figure 1, which correspond to two different ion−molecule clusters that can be associated with the connectivity schemes **1a** and **2a**, respectively. Ion **II**, whose connectivity corresponds to that of the experimentally observed species **1a**, is the most stable one, being 4.1 kcal mol^{-1} lower in energy than structure **III** and having a calculated binding energy of 13.6 kcal mol^{-1} with respect to the $HNO_3 + NO_2^+$ asymptote. The binding energy of **II** can also be evaluated by calculating the binding-energy difference between **II** and the $NO_2^+ \cdot H_2O$ cluster by means of the isodesmic ligand exchange reaction

$$HNO_3 + H_2ONO_2^+ \rightarrow H_3NO_3NO_2^+ + H_2O \quad (21)$$

TABLE 3: B3LYP 6-311G(d,p) Energies (au) and B3LYP 6-311++G(3df,3dp) Energies (in Parentheses) of Species Relevant to the $[HN_2O_5^+]$ System

species	*E*	*E* + ZPE	*H*(298 K)[a]
HNO_3	−280.967 372 (−281.000 037)	−280.940 916 (−280.973 581)	−280.936 446 (−280.969 111)
$H_2ONO_2^+$	−281.258 037 (−281.289 197)	−281.222 496 (−281.253 656)	−281.215 838 (−281.246 998)
$NO(OH_2)^+$	−281.235 322 (−281.265 574)	−281.196 430 (−281.226 682)	−281.191 801 (−281.222 053)
H_2O	−76.447 448 (−76.464 468)	−76.426 133 (−76.443 153)	−76.422 353 (−76.439 373)
NO_2^+	−204.773 270 (−204.795 337)	−204.761 473 (−204.783 540)	−204.757 875 (−204.779 942)
N_2O_5 (**I**)	−485.465 709 (−485.517 233)	−485.438 661 (−485.490 185)	−485.431 382 (−485.482 906)
II	−485.766 757 (−485.818 079)	−485.727 672 (−485.778 994)	−485.719 338 (−485.770 660)
III	−485.760 083 (−485.811 467)	−485.721 499 (−485.772 883)	−485.712 848 (−485.764 232)
IV (TS)	−485.751 909 (−485.799 519)	−485.715 026 (−485.762 636)	−485.706 827 (−485.754 437)

[a] Calculated by applying the thermal correction to 298 K.

TABLE 4: B3LYP 6-311++G(3df,3pd)//6-311G(d,p) Thermochemical Data (298 K) and Corresponding Experimental Values, kcal mol^{-1}

	computed values	experimental values
PA HNO_3	175.9	182.0 ± 2.3, ref 15
ΔPA HNO_3[a]	15.7	
$H_2O-NO_2^+$ BE	17.4	19.6 ± 2.4, ref 15
PA N_2O_5	182.0 (188.2)[b]	189.8 ± 2, this work
ΔPA N_2O_5	4.0	
$HNO_3-NO_2^+$ BE, **II**	13.6 (15.8)[b]	18.3 ± 2, this work
$HNO_3-NO_2^+$ BE, **III**	9.6	

[a] Difference between the PA of the alternative protonation sites of the molecule, see text. [b] Calculated from the computed $\Delta H°$ of the isodesmic reaction 21, utilizing the experimental $H_2O-NO_2^+$ BE and PA of HNO_3; see text.

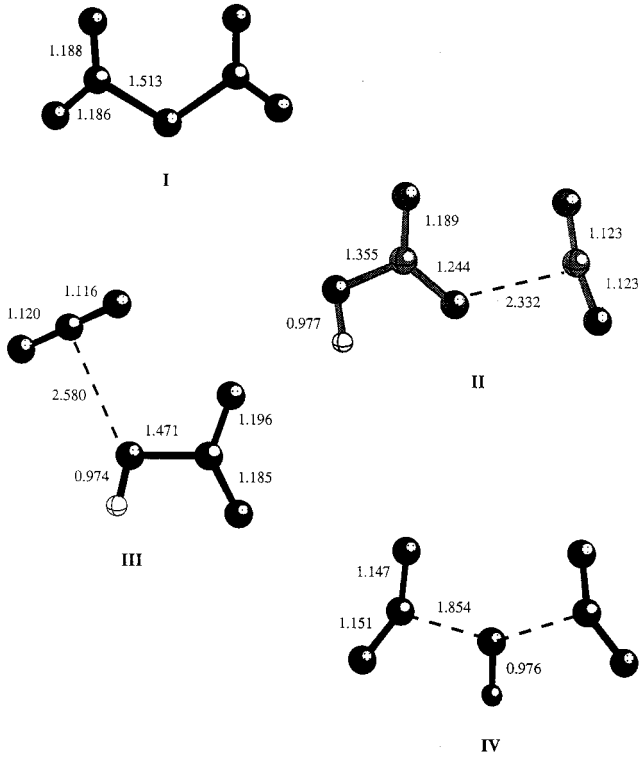

Figure 1. Optimized geometries of species relevant to the $[HN_2O_5]^+$ system. The numerals are the same as in Table 3.

Adding the calculated binding-energy difference to the experimental NO_2^+ BE of water, 19.6 ± 2.4 kcal mol^{-1}, the resulting BE for cluster **II** becomes 15.8 kcal mol^{-1}. Whereas both values are somewhat lower than the BE measured in this work, 18.3 ± 2 kcal mol^{-1}, the differences fall well within the range of the combined uncertainty.

The PA of N_2O_5 (see structure **I**) can similarly be computed both directly or from the computed enthalpy change of the isodesmic reaction 21, utilizing the experimentally determined value for HNO_3. The two approaches give values of 182.0 and 188.2 kcal mol^{-1}, respectively indicating that N_2O_5 has a larger proton affinity than HNO_3, consistent with the experimentally evaluated $PA(N_2O_5) = 189.8$ kcal mol^{-1}, reported in a previous paragraph. It can be observed that in both the **II** and **III** structures the two NO_2 groups are geometrically nonequivalent, whereas earlier in this paper they have been assumed to be chemically equivalent in structure **2a**, corresponding to **III**. The assumption remains valid, since the barrier to the exchange of the OH group between the two NO_2 in **III** (TS **IV**) was computed to be quite low, about 6 kcal mol^{-1}, confirming the correctness of the equivalence hypothesis under the experimental condition used.

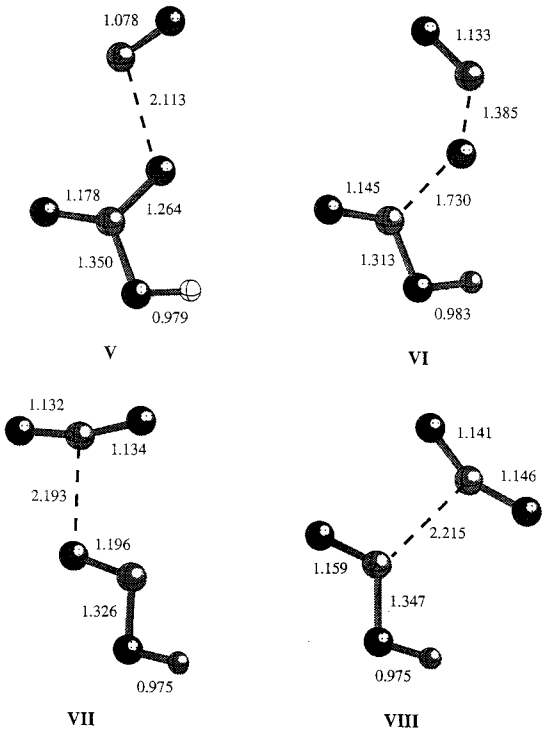

Figure 2. Optimized geometries of species relevant to the $[HN_2O_4]^+$ system. The numerals are the same as in Table 5.

$[HN_2O_4]^+$ Ions and N_2O_4 Isomers. We found a single stable $[HN_2O_4]^+$ ion, the NO^+/HNO_3 adduct, labeled as **V** (Figure 2), characterized by the connectivity of isomer **3**, in agreement with the experimental evidence (Tables 5 and 6). Despite extensive search, no minimum corresponding to the connectivity scheme **4** was found. The calculated NO^+ BE to HNO_3 amounts to 22.4 kcal mol^{-1} at 298 K, significantly larger than the experimental value from the kinetic method. This discrepancy appears to arise from a systematic overestimation of the computed NO^+ BE, which in the case of the $H_2O{\cdot}NO^+$ cluster

TABLE 5: B3LYP 6-311G(d,p) Energies (au) and B3LYP 6-311++G (3df,3dp)//6-311G(d,p) Energies (in Parentheses) of Species Relevant to the [$HN_2O_4^+$] System

species	*E*	*E* + ZPE	*H*(298 K)[a]
HNO_3	−280.967 372 (−281.000 037)	−280.940 916 (−280.973 58)	−280.936 446 (−280.969 111)
NO_2^+	−204.773 270 (−204.795 337)	−204.761 473 (−204.783 54)	−204.757 875 (−204.779 942)
NO^+	−129.571 275 (−129.583 798)	−129.565 591 (−129.583 798)	−129.562 286 (−129.574 809)
HNO_2	−205.761 768 (−205.786 430)	−205.741 476 (−205.786 470)	−205.737 301 (−205.762 003)
$HNO_3 + NO^+$	−410.538 647 (−410.583 835)	−410.506 507 (−410.583 835)	−410.498 732 (−410.543 920)
V	−410.579 911 (−410.670 757)	−410.546 304 (−410.620 757)	−410.538 728 (−410.579 574)
VI (TS)	−410.512 66 (−410.552 411)	−410.481 234 (−410.552 411)	−410.474 176 (−410.513 947)
VII	−410.564 239 (−410.606 588)	−410.530 279 (−410.606 588)	−410.522 809 (−410.565 158)
VIII	−410.556 545 (−410.598 205)	−410.522 715 (−410.598 205)	−410.515 304 (−410.556 964)
$HNO_2 + NO_2^+$	−410.535 038 (−410.581 807)	−410.502 949 (−410.581 807)	−410.495 176 (−410.541 945)
NO_2	−205.132 718 (−205.155 24)	−205.123 899 (−205.146 405)	−205.120 028 (−205.142 534)
IX	−410.289 34 (−410.332 054)	−410.265 893 (−410.308 607)	−410.259 641 (−410.302 355)
X	−410.269 818 (−410.313 626)	−410.248 496 (−410.292 304)	−410.241 634 (−410.285 442)

[a] Calculated by applying the thermal correction to 298 K.

TABLE 6: B3LYP 6-311++G(3df,3pd)//6-311G(d,p) Thermochemical Data (298 K) and Corresponding Experimental Values, kcal mol^{-1}

	computed values	experimental values
H_2O-NO^+ BE	25.3	18.5 ± 1.5, ref 39
HNO_3-NO^+ BE	22.4 (15.6)a	17.1 ± 2, this work
	Relative Energies	
$HNO_3 + NO^+$	0.0	
V	−22.4	
VI	18.8	
VII	−13.3	
VIII	−8.2	
$HNO_2 + NO_2^+$	1.2	
N_2O_4BE, **IX**	10.8	13.6, ref 41
N_2O_4, **X**	0.2	
PA N_2O_4, **IX**	166.4	
PA N_2O_4, **X**	186.1	
ΔPA N_2O_4, **X**	9.1	

[a] From the computed $\Delta H°$ of the isodesmic reaction 22, utilizing the experimental H_2O-NO^+ BE; see text.

is calculated to be 25.3 kcal mol^{-1}, vs the experimentally measured[19] value 18.5 ± 1.5 kcal mol^{-1} and the 19.5 kcal mol^{-1} value computed at the G2 level of theory.[40] However, the calculated NO^+ BE difference between water and nitric acid, corresponding to the enthalpy change computed for the ligand-exchange reaction

$$HNO_3{\cdot}NO^+ + H_2O \rightarrow H_2O{\cdot}NO^+ + HNO_3 \qquad (22)$$

amounts to 2.9 kcal mol^{-1}, which combined with the experimental NO^+ BE of water, leads to a NO^+ BE of HNO_3 of 15.6 kcal mol^{-1}, quite compatible with the experimental value from the kinetic method.

We also studied the potential energy surface for the oxygen-transfer reaction

$$NO^+ + HNO_3 \rightarrow NO_2^+ + HNO_2 \qquad (23)$$

the overall process whose occurrence is revealed by the NO_2^+ loss in the CAD spectrum of **3**. Whereas the process is found to be almost thermoneutral, being endothermic by ca. 1.2 kcal mol^{-1}, it requires overcoming a sizable energy barrier, since the transition state **VI** is located 18.8 kcal mol^{-1} higher than the reactants. This is again consistent with the small intensity found for the NO_2^+ peak in the CAD spectra. On the product side of the potential energy surface, the two structures **VII** and **VIII** (Figure 3) were found that correspond to two NO_2^+. HNO_2 clusters.

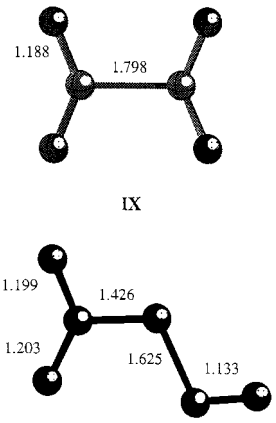

Figure 3. Optimized geometries of isomeric N_2O_4 oxides. The numerals are the same as in Table 5.

The computed energies of **V** and **VII** can be used to determine the proton affinities of the [N_2O_4] oxides. Two N_2O_4 isomers are known to exist, the more stable symmetric O_2N-NO_2 isomer **IX** and the asymmetric O_2N-ONO isomer **X**, which has been isolated in the condensed phase only. We computed the stability of the two molecules with respect to their dissociation into two NO_2 molecules to be 10.8 and 0.2 kcal mol^{-1}, respectively, at 298 K. The reported experimental value for **IX** is 13.6 kcal mol^{-1},[41] whereas none is available for **X**. Stirling et al.,[42] who studied several nitrogen oxides using both local and gradient-corrected density functional theory, obtained a binding energy of 4.7 kcal mol^{-1} for the asymmetric isomer using the Becke−Perdew nonlocal functional with the TZP basis set (BP/TZP). On the other hand, the BP/TZP level overestimates the binding energy of the symmetric isomer by 5 kcal mol^{-1}, so we believe that the correct value for **X** is actually lower and closer to ours. Furthermore, both the N_2O_5 and N_2O_4 geometries obtained at the B3LYP/6-311G(d,p) level are closer to the experimental ones than those obtained at BP/TZP level. However, these minor discrepancies do not affect the conclusion that asymmetric N_2O_4 is extremely unstable in the gas phase.

The $-\Delta H°$ of the protonation process yielding **VIII**, corresponding to the proton affinity for symmetric N_2O_4, is calculated to be 166.4 kcal mol^{-1}, i.e., 15.8 kcal mol^{-1} smaller than that of N_2O_5. If the asymmetric N_2O_4 is protonated on the NO_2 group, cluster **V** is the resulting product, whereas if protonation occurs on the terminal oxygen of the ONO group cluster **VII** is formed. The resulting local proton affinities were computed to be 186.1 and 177.0 kcal mol^{-1}, respectively.

Conclusions

The salient feature of the coherent picture outlined by the mutually supporting computational and experimental results is the formation of electrostatically bound clusters as the most stable adducts from the gas-phase reaction of nitric acid with the NO_2^+ and NO^+ cations. In both cases, the coordination occurs preferentially with the nitro, rather than the OH, group of HNO_3. Focusing attention on the nitration process, the behavior of NO_2^+ stands in contrast with that of H^+, whose attack on the OH group of HNO_3 is energetically favored by some 20 kcal mol^{-1}.[12] Such a different behavior of the two cations can be rationalized by observing that NO_2^+ forms electrostatically bound complexes with HNO_3, whereas the attack of H^+ leads to formation of new covalent bonds, and hence the process yielding the most stable molecule, H_2O, is favored. Thus, the factors controlling the stability of the reaction products are different in the case of protonation and nitration. In the latter process, the dominating factor appears to be the ion−dipole interaction, leading to the preferential coordination of NO_2^+ to the negative end of the HNO_3 dipole, namely, the nitro group. On the other hand, consistent with the conclusions of Lee and Rice,[12,13] the competition for the proton between the basic sites of HNO_3 is controlled by the relative stability of the covalent bonds formed. Similar considerations seem to apply to related nitration processes involving methyl nitrate, ethyl nitrate, and nitramide, whose mass spectrometric study provides strong evidence for the formation of ionic clusters where NO_2^+ is preferentially coordinated to the nitro group, and to the nitrosation of HNO_3.

Turning to the main problem addressed in the present study, the theoretical and experimental evidence concur in demonstrating the higher PA of the nitro group than of the central O atom of N_2O_5, and the relatively large PA of the latter, exceeding that of HNO_3 and, by a wide margin, that of H_2O. This is of interest, suggesting that protonation of N_2O_5 by H_3O^+ or $H_2NO_3^+$ ions can indeed represent the first step of the decomposition of dinitrogen pentoxide in atmospheric ionic clusters and aerosols.

Furthermore, the almost thermoneutral character and the sizable, but not prohibitively high, energy barrier to the oxygen-transfer process (reaction 23) are of potential interest to atmospheric chemistry, pointing to the possible occurrence of a hitherto neglected intracluster reorganization reaction.

As a final remark the present study seems to confirm the predictive value of the correlation between the PA of n-type nuclephilic centers and the NO^+ [34] or NO_2^+ [24] BE, whose validity has been verified to a satisfactory degree of accuracy by the theoretical and experimental results.

Experimental Section

All gases used in the chemical ionization (CI) experiments were purchased from Matheson Gas Products Inc. with a stated purity in excess of 99.95 mol %. The chemicals were research-grade products from Aldrich Chemical Co. or synthesized and purified according to standard procedures. Nitramide was obtained by methanolysis of *N*-nitroacetamide,[43] prepared in turn by NO_2BF_4 nitration of acetamide. Dinitrogen pentoxide was synthesized by the technique of Davidson et al.,[44] which involves oxidation of NO by O_3, generated by passing UHP grade oxygen (Matheson 99.95%) through a commercial ozonizer. The MIKE spectra were recorded using a ZAB-2F mass spectrometer from VG Micromass Ltd., whose CI source, fitted with a specially built cooling system, was operated at temperatures ranging from 40 to 50 °C. Typical operation conditions were as follows: accelerating voltage 8 kV, emission current 1 mA, repeller voltage 0 V, electron energy 50 V. The FT-ICR experiments were performed utilizing a 47e APEX spectrometer from Bruker Spectrospin AG, equipped with an external ion source operated at total pressures not exceeding 7×10^{-5} Torr.

Acknowledgment. This work was supported by the University of Rome "La Sapienza" and the Italian National Research Council (CNR). The authors are indebted to Fausto Angelelli for the FT-ICR measurements.

Supporting Information Available: Cartesian coordinates of the relevant stationary points for structures **I**−**X** (3 pages). Ordering and accessing information is given on any current masthead page.

References and Notes

(1) Eberson, L.; Hartshorn, M. P.; Radner, F. *Acta Chem. Scand.* **1994**, *48*, 937 and references therein.
(2) Fehsenfeld, F. C.; Ferguson, E. E. *Geophys. Res.* **1969**, *74*, 2217.
(3) Ferguson, E. E.; Fehsenfeld, F. C.; Albritton, D. L. *Gas-Phase Ion Chemistry*; Bowers, M. T., Ed.; Academic Press: New York, 1979; Vol. 1, Chapter 2.
(4) Brasseur, G.; Solomon, S. *Aeronomy of the Middle Atmosphere*; D. Reidel: Dordrecht, 1986.
(5) Böhringer, H.; Fahey, D. W.; Fehsenfeld, F. C.; Ferguson, E. E. *Planet. Space Sci.* **1983**, *31*, 185.
(6) Fehsenfeld, F. C.; Ferguson, E. E. *J. Chem. Phys.* **1973**, *59*, 6272.
(7) Fehsenfeld, F. C.; Howard, C. J.; Schmeltekopf, A. L. *J. Chem. Phys.* **1975**, *63*, 2835.
(8) Kay, B. D.; Herman, V.; Castleman, A. W., Jr. *Chem. Phys. Lett.* **1981**, *80*, 469.
(9) Nguyen, M.-T.; Hegarty, A. F. *J. Chem. Soc., Perkin Trans. 2* **1984**, 2043.
(10) (a) Cacace, F.; Attinà, M.; de Petris, G.; Speranza, M. *J. Am. Chem. Soc.* **1990**, *112*, 5841. The structural assignment, based on the interpretation of the MIKE and CAD spectra of $H_2NO_3^+$ has been confirmed very recently by vibrational spectroscopy; see: (b) Choi, J. H.; Kuwata, K. T.; Cao, Y.-B.; Haas, B.-M.; Okumura, M. *J. Phys. Chem.* **1997**, *101*, 6753.
(11) Cacace, F.; Attinà, M.; de Petris, G.; Speranza, M. *J. Am. Chem. Soc.* **1990**, *112*, 1041.
(12) Lee, T. J.; Rice, J. E. *J. Phys. Chem.* **1992**, *96*, 650.
(13) Lee, T. J.; Rice, J. E. *J. Am. Chem. Soc.* **1992**, *114*, 8247.
(14) Sunderlin, L. S.; Squires, R. R. *Chem. Phys. Lett.* **1993**, *212*, 307.
(15) Cacace, F.; Attinà, M.; de Petris, G.; Speranza, M. *J. Am. Chem. Soc.* **1994**, *116*, 6413.
(16) Zhang, X.; Mereand, E. J.; Castleman, A. W., Jr. *J. Phys. Chem.* **1994**, *98*, 3554.
(17) Cao, Y.; Choi, J.-C.; Haas, B.-M.; Okamura, M. *J. Phys. Chem.* **1994**, *98*, 12176.
(18) Bush, A. M.; Dyke, J. M.; Wright, T. G. *J. Chem. Phys.* **1997**, *106*, 6031.
(19) Bernardi, F.; Cacace, F.; Grandinetti, F. *J. Chem. Soc., Perkin Trans. 2* **1989**, 413.
(20) de Petris, G. *Org. Mass Spectrom.* **1990**, *25*, 83.
(21) Ricci, A. *Org.Mass Spectrom.* **1994**, *29*, 53.
(22) Aschi, M.; Cacace, F.; de Petris, G.; Pepi, F. *J. Phys. Chem.* **1996**, *100*, 16532.
(23) Attinà, M.; Cacace, F.; Ciliberto, E.; de Petris, G.; Grandinetti, F.; Pepi, F.; Ricci, A. *J. Am. Chem. Soc.* **1993**, *115*, 12398.
(24) Cacace, F.; de Petris, G.; Pepi, F.; Angelelli, F. *Proc. Natl. Acad. Sci. U.S.A.* **1995**, *92*, 8635.
(25) Liuti, G.; Dondes, S.; Harteck, P. *J. Phys. Chem.* **1968**, *72*, 1081.
(26) Jochims, H.-W.; Denzer, W.; Baumgärtel, H.; Lösking, O.; Willner, H. *Ber. Bunsen-Ges. Phys. Chem.* **1992**, *96*, 573.
(27) O′Connor, C. S. S.; Jones, N. C.; O′Neale, K.; Prince, S. D. *Int. J. Mass Spectrom. Ion Processes* **1996**, *154*, 203.
(28) Trush, B. A. *Rep. Prog. Phys.* **1988**, *51*, 1341 and references therein.
(29) Guttzen, P. J.; Arnold, F. *Nature* **1986**, *324*, 651.
(30) Hu, J. H.; Abbott, J. P. D. *J. Phys. Chem.* **1997**, *101*, 871.
(31) Cooks, G. R.; Patrick, J. S.; Kotiaho, T.; McLuckey, S. A. *Mass Spectrom. Rev.* **1994**, *13*, 287.
(32) Occurrence of isomerization processes and selective stabilization of a charged species within ion−neutral complexes are well-established, cf.: (a) Longevialle, P. *Mass Spectrom. Rev.* **1992**, *11*, 157. (b) Brutschy, B. *Chem. Rev. (Washington, D.C.)* **1992**, *92*, 1567 and references therein.
(33) de Petris, G.; Pepi, F. Submitted for publication in *Chem. Phys. Lett.*

(34) Cacace, F.; de Petris, G.; Pepi, F. *Proc. Nat. Acad. Sci. U.S.A.* **1997**, *94*, 3507.
(35) Becke, A. D. *J. Chem. Phys.* **1993**, *98*, 5648.
(36) Lee, C.; Yang, W.; Parr, R. G. *Phys. Rev. B* **1988**, *37*, 785.
(37) Smith, B. J.; Radom, L. *Chem. Phys. Lett.* **1994**, *231*, 345.
(38) Frisch, M. J.; Trucks, G. W.; Schlegel, H. B.; Gill, P. M. W.; Johnson, B. G.; Robb, M. A.; Cheeseman, J. R.; Keith, T.; Petersson, G. A.; Montgomery, J. A.; Raghavachari, K.; Al-Laham, M. A.; Zakrzewski, V. G.; Ortiz, J. V.; Foresman, J. B.; Cioslowski, J.; Stefanov, B. B.; Nanayakkara, A.; Challacombe, M.; Peng, C. Y.; Ayala, P. Y.; Chen, W.; Wong, M. W.; Andrés, J. L.; Replogle, E. S.; Gomperts, R.; Martin, R. L.; Fox, D. J.; Binkley, J. S.; Defrees, D. J.; Baker, J.; Stewart, J. P.; Head-Gordon, M.; Gonzales, C.; Pople, J. A. *Gaussian 94*, Revision D.3; Gaussian, Inc.: Pittsburgh, PA, 1995.
(39) French, M. A.; Hills, L. P.; Kebarle, P. *Can. J. Chem.* **1973**, *31*, 456.
(40) Aschi, M.; Grandinetti, F. *Chem. Phys. Lett.* **1996**, *258*, 12.
(41) Vosper, A. J. *J. Chem. Soc.* **1970**, 625.
(42) Stirling, A.; Papai, I.; Mink, J.; Salahub, D. R. *J. Chem. Phys.* **1994**, *100*, 2910.
(43) Andrev, S. A.; Lebedev, B. A.; Tselinskii, I. V. *Zh. Org. Khim.* **1978**, *14*, 2513.
(44) Davidson, J. A.; Viggiano, A. A.; Howard, C. J.; Dotan, I.; Fehsenfeld, F. C.; Albritton, D. L.; Ferguson, E. E. *J. Chem. Phys.* **1978**, *68*, 2085.